การตอบสนองของคลื่นแม่เหล็กไฟฟ้าที่ระยะเวลาที่เปลี่ยนไป ในการเฝ้าติดตามการกักเก็บก๊าซคาร์บอนไดออกไซด์ในชั้นหินกักเก็บ

นางสาวแพรวผกา ชุมทอง
เลขประจำตัวนิสิต 513 27383 23

รายงานนี้เป็นส่วนหนึ่งของการศึกษาตามหลักสูตรปริญญาตรี
สาขาวิชาธรณีวิทยา ภาคธรณีวิทยา คณะวิทยาศาสตร์
จุฬาลงกรณ์มหาวิทยาลัย
ปีการศึกษา 2554

CONTROLLED-SOURCE ELECTROMAGNETIC FOR 4D-MONITORING OF CO_2 STORAGE IN A GEOLOGICAL RESERVOIR

Ms. Praewpaka Chumtong

ID: 513 27383 23

A REPORT SUBMITTED IN PARTIAL FULFILLMENT OF THE REQUIREMENTSFOR THE DEGREE OF BACHELOR OF SCIENCE

DEPARTMENT OF GEOLOGY, FACULTY OF SCIENCE

CHULALONGKORN UNIVERSITY

2011

__/__/__

Date of submit

__/__/__

Date of approval

.....

(Dr. Thanop Thitimakorn)

Senior Project Advisor

การตอบสนองของคลื่นแม่เหล็กไฟฟ้าที่ระยะเวลาที่เปลี่ยนไปในการเฝ้าติดตามการกักเก็บก๊าซคาร์บอนไดออกไซด์ในชั้นหินกักเก็บ

นางสาวแพรวผกา ชุมทอง

ภาควิชาธรณีวิทยา คณะวิทยาศาสตร์ จุฬาลงกรณ์มหาวิทยาลัย

โทรศัพท์ : 0-8310-3473, อีเมล์: chumtong.p@hotmail.com

บทคัดย่อ

ในการผลิตน้ำมันและก๊าซให้ได้มากที่สุดหรือการกักเก็บก๊าซคาร์บอนไดออกไซด์ในชั้นหินกักเก็บจำเป็นต้องอาศัยความรู้เกี่ยวกับคุณสมบัติของชั้นหินกักเก็บเพื่อที่จะเฝ้าติดตามการเปลี่ยนแปลงของของเหลวหรือก๊าซภายในชั้นหินกักเก็บนั้น ความแตกต่างของคุณสมบัติทางไฟฟ้าของของเหลวที่แตกต่างกันในชั้นหินเช่น ระหว่างก๊าซหรือน้ำมันกับน้ำ จะทำให้การสำรวจโดยใช้คลื่นแม่เหล็กไฟฟ้าเป็นวิธีที่มีประสิทธิภาพในการเฝ้าวิเคราะห์การเปลี่ยนแปลงภายในชั้นหินกักเก็บ ในงานวิจัยครั้งนี้ เราได้ทำการสร้างแบบจำลองของชั้นหินกักเก็บขึ้นมาโดยอ้างอิงข้อมูลของรูพรุนและค่าการซึมผ่านได้มาจากงานวิจัยซึ่งทำการศึกษาลักษณะศิลาวรรณนาของชั้นหินกักเก็บในบริเวณพื้นที่กวาว่า ประเทศซาอุดิอาระเบีย จากนั้นเราได้จำลองการเปลี่ยนแปลงของของเหลวภายในชั้นหินจากเริ่มต้นที่เป็นน้ำ แล้วทำการอัดก๊าซคาร์บอนไดออกไซด์เข้าไปแทนที่เป็นระยะเวลาต่อเนื่อง 10 ปี นำค่าข้อมูลที่ระยะเวลาต่างๆมาคำนวณให้เป็นแบบจำลองชั้นหินในรูปของค่าความนำไฟฟ้า จากนั้นทำการคำนวณค่าของคลื่นแม่เหล็กไฟฟ้าที่ระยะเวลาต่างๆโดยจะขึ้นอยู่กับตัวแปรสองชนิดคือ ความถี่ของสัญญาณและความลึกของชั้นหินกักเก็บที่อยู่ในพื้นดิน จากการศึกษาพบว่า คลื่นแม่เหล็กไฟฟ้าที่เปลี่ยนแปลงไปมีค่าน้อยแต่ยังสังเกตและวัดค่าได้ซึ่งความแตกต่างของคลื่นแม่เหล็กไฟฟ้าเป็นผลมาจากการที่ภายในชั้นหินกักเก็บมีค่าความนำไฟฟ้าที่เปลี่ยนแปลงไปนั่นเอง จากการวิเคราะห์ผลพบว่าคลื่นแม่เหล็กไฟฟ้าสามารถตรวจจับการเปลี่ยนแปลงคุณสมบัติของชั้นหินกักเก็บที่เปลี่ยนแปลงไปได้ ซึ่งทำการวิเคราะห์ผลหลังจากเริ่มอัดก๊าซคาร์บอนไดออกไซด์ลงไป 1.5 ปี, 3 ปี, 6 ปี, และ 10 ปี ที่ระดับความลึกของชั้นหินกักเก็บ 250 เมตร, 500 เมตร และ 1000 เมตร ตามลำดับ เราพบว่ายิ่งสัญญาณมีความถี่สูงขึ้นจะทำให้ความชัดเจนของคลื่นแม่เหล็กไฟฟ้าเพิ่มขึ้น อย่างไรก็ตามความละเอียดจะลดลงเมื่อชั้นหินอยู่ลึกขึ้น

Key words: Controlled-Source Electromagnetic, CO_2 Storage, 4D-monitoring

Controlled-Source Electromagnetic for 4D-monitoring of CO_2 Storage in a Geological Reservoir

Praewpaka Chumtong,

Department of Geology, Faculty of Science, Chulalongkorn University

Tel: 0-2612-1196, E-mail: chumtong.p@hotmail.com

Abstract

Maximizing oil and gas production, or CO_2 sequestration capacity of a reservoir, requires detailed knowledge of reservoir properties and monitoring changes in fluid or gas content. Large contrasts of electrical resistivity between different fluids (gas/oil versus brine/connate water) and reservoir rocks make 4D controlled-source electromagnetic (CSEM) monitoring an effective tool for reservoir analysis. To examine the feasibility of CSEM monitoring at the Ghawar oil field, Saudia Arabia, we use porosity and permeability data from the Ghawar field to construct a geologic model of the reservoir. We simulate changes in water and CO_2 gas content within the reservoir over ten years in a CO_2 injection scenario. Archie's law for carbonate reservoirs is then used to convert the simulation results to changes of reservoir conductivity. Last, the reservoir is embedded within a 3D homogenous seabed background conductivity model. A Finite Element Modeling technique is used to simulate time-lapse frequency domain CSEM data for reservoirs buried at a variety of depths. The results of the feasibility study show that the CSEM response exhibits small but measurable changes that are characteristic of reservoir-depletion geometry (conductivity). Our analysis demonstrates that CSEM can detect changes in reservoir properties at 1.5 years, 3 years, 6 years, and 10 years at 250m, 500m, and 1000m depths respectively. Moreover, high frequency sources result in better resolution, though resolution degrades significantly with reservoir depth.

Key words: Controlled-Source Electromagnetic, CO_2 Storage, 4D-monitoring

Acknowledgements

I would like to express my gratitude to all of those who gave me the chance to work on and complete this project. I have to thank my advisor Dr. Thanop Thitimakorn for his guidance, encouragement, valuable supervision through this study. I have furthermore to thank the Department of Geophysics, Stanford University, for providing me a chance to do the research work and use department data.

I am deeply indebted to my co-advisors Dr. Armando Sena, Dr. Youli Quan, and Prof. Jerry Harris from Stanford University whose help, stimulating suggestions, and encouragement helped me over the course of the summer. I also would like to thank my PA, Daniel Sinnett, for all his help and guidance.

I thank to Department of Geology, Chulalongkorn University for supporting me a chance to attend SURGE program at Stanford University, and also thank to Chevron Thailand Exploration and Production, Ltd. for funding.

Especially, I would like to give my special thanks to my parents whose patient love enabled me to complete this project.

CONTENTS

Page

LIST OF FIGURES

Page

CHAPTER I

INTRODUCTION

1.1 General Statement

Global atmospheric concentration of CO_2 is 36% higher than it was before the industrial revolution (EPA, 2007) (Figure 1.1). This rise in atmospheric CO_2 is the primary contributor to currently observed increases in global atmospheric and ocean temperatures. Mitigation of future global warming requires the reduction of emissions and long-term storage of CO_2. One technique available for long-term CO_2 storage is CO_2 sequestration within hydrocarbon reservoirs and saline aquifer.

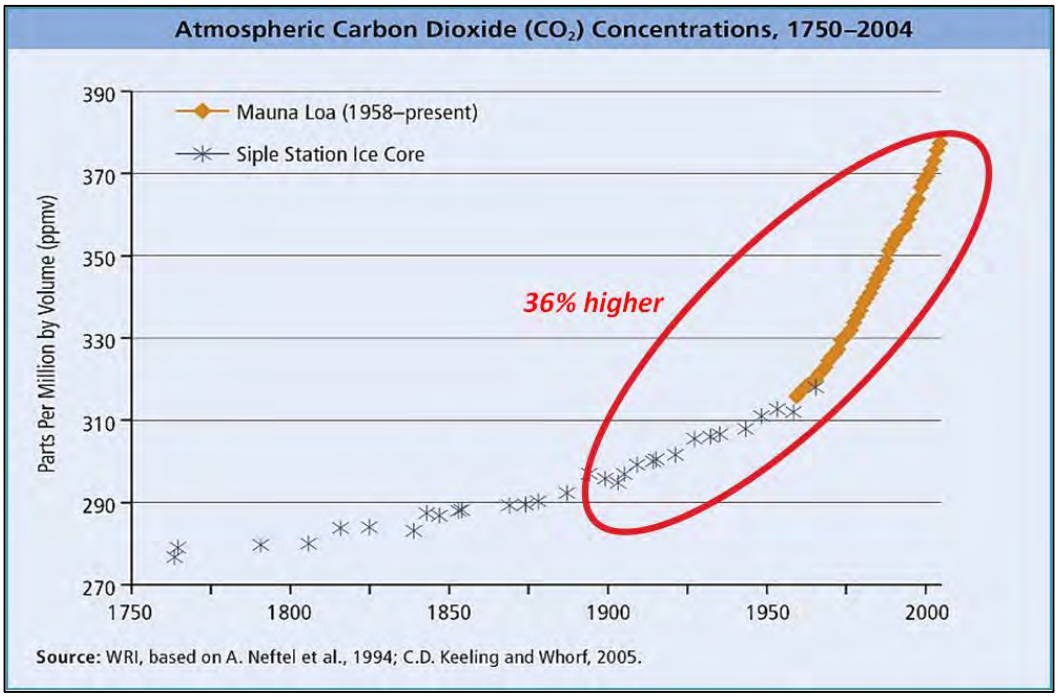

Figure 1.1: Global atmospheric Carbon Dioxide concentrations.

< http://www.earthtrendsdelivered.org/node/38>

Moreover, CO_2 is also used for enhanced oil recovery (EOR). CO_2 EOR can also sequester a certain amount of hydrocarbon in the reservoir. As a result, CO_2 EOR not

only reduces net green gas emissions considerably, but also increases oil production (Figure 1.2).

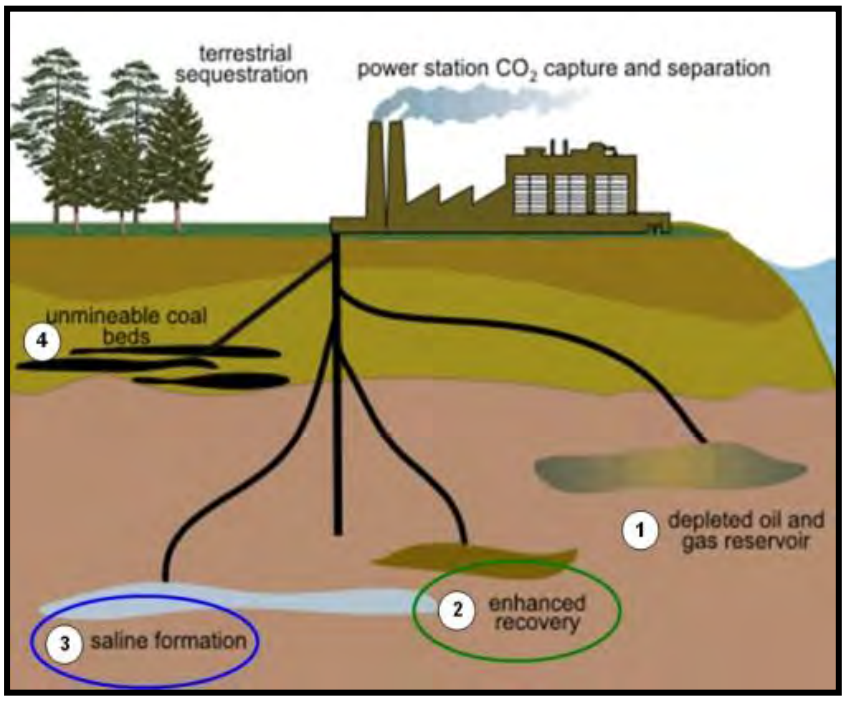

Figure 1.2: CO_2 storage.

<http://coreenergyholdings.com/GeologicCO2Sequestration.html>

The future of the oil industry is centered on our ability to extract more oil out of existing reservoirs. A problem involving CO_2 emissions and climate change can be turned into an opportunity if managed properly. Each EOR project involving CO2 flooding is in-effect a sequestration process as a high percentage of CO2 remains in the ground. Monitoring is required for both sequestration and EOR and we need to understand how this process can be improved through closer integration of engineering and geosciences (Davis, T., 2011).

The electrical and magnetic properties of the subsurface, including electrical permittivity $\in$, magnetic permeability μ , and conductivity σ vary from material to material. These quantities are indicative of various properties of the material including the availability and mobility of free electrons and the ease with which the material may become magnetized or electrically polarized. In turn, these properties can be related to

less abstract geological conditions, such as lithology, porosity, permeability, and structure. It is the duty of the electromagnetic geophysicist to measure the electromagnetic properties remotely, and to interpret the measured data in order to characterize the subsurface.

Conductivity is the most variable of the electromagnetic properties of typical earth materials, which range from highly conductive metallic ore minerals, to slightly conductive crystalline minerals such as quartz. In fact, conductivity within the Earth spans 20 orders of magnitude. Despite this great range, it is often difficult to relate measured conductivity to lithology. That is, if the conductivity of a region of the subsurface is known, the lithology of that region is not necessarily known. Porosity and permeability (and thus water content), for example, often dwarf the contribution of the actual mineral chemistry to the average conductivity, causing what may normally be a poorly conductive (when dry) mineral appear to be several orders of magnitude more conductive than it actually is (Grant and West, 1965).

A variety of methods have been developed to remotely measure the conductivity (or its reciprocal, resistivity) of the subsurface. Direct current (DC) resistivity, induced polarity (IP), spontaneous potential (SP), controlled-source induction (CSEM), and magnetotelluric induction (MT) are the most commonly used. CSEM offers several advantages over direct current resistivity surveys: less manpower is required, and larger areas may be surveyed within the same amount of time (McNeill, 1980a).

The Controlled-Source Electromagnetic (CSEM) technique has been used to find and evaluate hydrocarbon reservoirs. The electrical conductivity contrast between hydrocarbon- and saline water-saturated rocks causes anomalies in the measured electric field. This makes the CSEM method a useful geophysical tool for identifying hydrocarbon reservoirs (e.g. Edidesmo, et al., 2002) and estimating reservoir size, extent, and properties.

The CSEM method was originally developed for mining applications in which conductive ore bodies form excellent, compact targets within resistive host crystalline rocks. The CSEM method is also able to identify conductive fracture zones in crystalline

bedrock aquifers for groundwater prospecting applications. However, generic geological site characterization problem is very difficult. The subsurface geology contains quasi-localized features such as the weathered mantle, bedrock, bedding planes, faults, joints, and fracture zones in addition to continuously distributed textural and compositional variations. It is the difficult task of the EM geophysicist to interpret such CSEM responses in terms of the subsurface geology with its attendant spatial complexity. The presence of man-made conductors in the subsurface adds to the difficulty (Stalnaker, J.L., 2002).

Time-lapse CSEM consists of repeated surveys of a reservoir to monitor changes in reservoir conductivity, and thus fluid content. 4D transient EM monitoring can detect gas reservoirs and monitor changes in gas and water content due to pumping (Wright et al., 2002). Furthermore, the feasibility of using CSEM to determine the lateral extent and thickness of resistive bodies (e.g. hydrocarbon reservoirs) has been demonstrated (Constable and Weiss, 2006).

1.2 Term Defined

Controlled-Source Electromagnetic (CSEM) method

The controlled-source electromagnetic method (CSEM) is well established in geophysical prospecting. The CSEM method involves energizing the electrically conducting earth with an inductively coupled or directly coupled time-varying source of current and measuring with coincident or remote receivers the secondary electromagnetic (EM) field caused by the resulting eddy currents. The secondary field, at frequencies where the displacement current is negligible, depends primarily on the electrical conductivity distribution of the ground (Eugene et al., 2001) (Figure1.3).

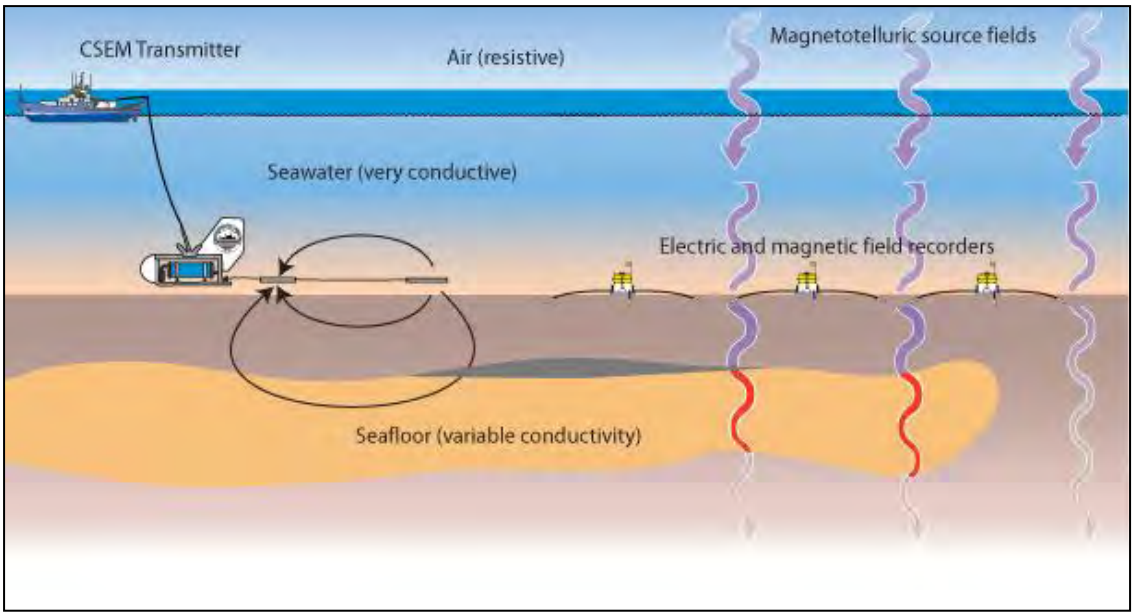

Figure 1.3: CSEM acquisition. <http://marineemlab.ucsd.edu>

1.3 Objectives

1. Study Controlled-Source Electromagnetic (CSEM) responses to changes in CO_2 saturation
2. study the feasibility of using Controlled-Source Electromagnetic (CSEM) to monitor CO_2 stored in the reservoir
3. Determine what signatures exhibit sensitivity to changes in CO_2 saturation

1.4 Scope of Work

This project presents a feasibility study of 4-D CSEM as a prelude to conduct a field study on monitoring CO_2 injection. Of particular interest is the sensitivity of CSEM to reservoir depth and signal frequency. We examine changes in the magnitude of CSEM responses due to displacement of water by CO_2 in 10 year of CO_2 sequestration scenario as a function of reservoir depth and CSEM source frequency. We create the simulated reservoir based on geological data of Ghawa field, Saudi Arabia.

1.5 Source of Data

To study the CSEM response due to CO_2 injection, we demonstrate the CSEM response of a carbonate reservoir in Ghawar field, Saudi Arabia which is acquire the data of the location from available research, Origin of Dolomite in the Arab-D Reservoir from the Ghawar Field, Saudi Arabia: Evidence from Petrographic and Geochemical Constraints (Swart et al., 2005).

The Arab-D reservoir which is a carbonate reservoir in the Ghawar Field of Saudi Arabia (Figure 1.4) is the world's largest oil field producing approximately 5 million barrels a day (Durham, 2005)

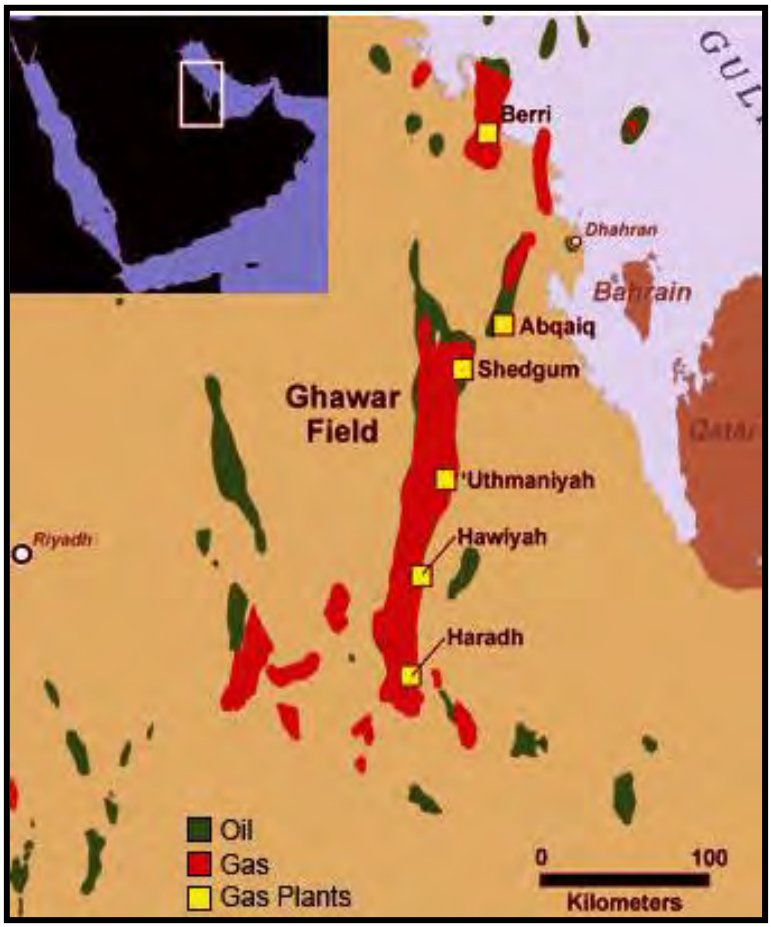

Figure 1.4: Source of data of the study area, Ghawar oil field, Saudi Arabia.

<http://www.energyandcapital.com/articles/ghawar-oil-saudi/253>

1.6 Expected Result

CSEM will response to changes in saturation in the model I have created. Higher given source frequency will give a better resolution and resolution will decrease with depth of the reservoir.

CHAPTER II

LITERATURE REVIEWS AND THEORY

2.1 Literature Reviews

In this study the literature review is focused on the process of CSEM method in order to get the CSEM responses.

Wright et al. (2002) presented time-lapse transient EM surveys over a shallow underground gas storage reservoir with high porosity and showed that the data is repeatable enough to detect the reservoir and monitor the moving of gas-water content due to gas pumping and/or extracting in summer and winter, respectively.

Previous studies implied the feasibility of CSEM for reservoir monitoring by showing that CSEM responses are sensitive to the lateral extent and thickness of resistive bodies (Constable and Weiss, 2006). Of particular interest is the sensitivity of CSEM to the edges of a resistive body embedded in amore conductive surrounding medium, which is directly relevant to offshore reservoir monitoring.

Lien and Mannseth (2008) conducted a feasibility study of time-lapse CSEM data to monitor the waterflooding of an oil reservoir. Utilizing 3D integral equation modeling, they found that time-lapse signals exhibit detectable changes in the present of measurement errors. Orange et al. (2009) further expanded the work by Lien and Mannseth (2008) by utilizing a 2D finite element modeling to simulate time-lapse CSEM data in response to several simplified waterflooding scenario, including lateral and bottom flooding, and partial depletion. Through a set of 2D modeling studies, they showed that a repeatability of 1-2% is required to detect the small time-lapse modeling by perturbing conductivity over a large reservoir (10*10 km^2) and reported anomalies of 30%-50% changes in relative amplitudes of base and monitor surveys.

Previous studies implied the feasibility of CSEM for reservoir monitoring by showing that CSEM responses are sensitive to the lateral extent and thickness of resistive bodies (Constable and Weiss, 2006). Of particular interest is the sensitivity of

CSEM to the edges of a resistive body embedded in amore conductive surrounding medium, which is directly relevant to offshore reservoir monitoring. They mentioned that these relatively strong time-lapse signal as well as different shapes of fronts can be monitored considering 5% repeatability for time-lapse surveys.

Black et al. (2009) modeled time-lapse CSEM response over a realistic geologic model but simplified flood geometry without fluid flow simulation and rock physics modeling. They showed that marine CSEM data is able to locate the position of oil-water contact if the field is normalized by the background, bathymetry, and salt dome effects. No reservoir simulations were performed in above-mentioned studies; instead, they all consider direct perturbation of electrical-conductivity.

In 2009, PGS (Petroleum Geo-Services) published a time-domain EM repeatability experiment over the North Sea Harding field. Fluid flow simulation and resistivity modeling by Archie's equation for clay-free sandstone were combined by integral equation modeling to simulate EM data. They concluded that the production-induced time-lapse changes in reservoir resistivity would be observable provided that a signal to noise ratio of greater than 100, i.e., 40dB is obtained.

Lien and Mannseth (2008) consider this problem using 3D integral-equation modeling and find that indeed the time-lapse CSEM signal exhibits measureable changes in response to reservoir production.

Michael A. F. and Sofia D. (2009) studied the applicability and resolution power of low-frequency Controlled-Source Electromagnetic (CSEM) data in shallow and deep water environments are studied on typical CSEM benchmark models. They apply the fast and accurate 3D finite-difference (FD) modeling code. They showed that use of low-frequency ($f<0.05$ Hz) electromagnetic measurements can overcome the airwave effect, allowing CSEM technology to be effectively used in shallow water to resolve deep 3D resistive targets.

Here, we first generate a 3D geological reservoir model showing the realistic spatial distribution of petrophysical parametrers. Fluid flow simulation and a geologically consistent rock physics model are then employed to convert the petrophysical

properties of the carbonate rock to electrical resistivity. The representative time-dependent resistivity model developed here shows the accurate front geometry during a CO_2 injection to storage in the reservoir. To simulate the surrounding rocks, we buried the reservoir into a 3D background resistivity model. Finally, we numerically acquire 1D time-lapse CSEM data over the reservoir to study the scenario of EM anomalies in monitoring of CO_2 injection scenario. To the best knowledge, no such comprehensive study has been reported in the open literature.

2.2 Theory

2.2.1) Rock Physics: Electric Properties of Porous Media

Rock Physics modeling can transform the petrophysical properties of a reservoir to rock conductivity, which can be further used to simulate CSEM data. This process is an essential step in any inversion project aimed at estimating petrophysical properties. In CSEM reservoir monitoring, fluid flow simulation, rock physics, and CSEM forward modeling can be effectively combined to simulate CSEM data and, ultimately, to predict reservoir properties. Archie's equation (Archie 1942) has been widely used in geosciences community to relate petrophysical properties of reservoir rocks to electrical conductivity.

Archie's equation

Archie (1942) shows experimentally a simple relationship between the formation factor of a completely water-saturated sedimentary rock and the porosity of the rock, and introduces the equation

$$F = \frac{1}{\varphi^m} \tag{2.1}$$

where F is formation factor, φ is porosity, and m is the cementation factor. .Archie (1942) postulated that m depends on cementation. The formation factor F is the resistivity of a fully water-saturated rock R_0, divided by the resistivity of the water R_w:

$$F = \frac{R_0}{R_w} \tag{2.2}$$

Archie's equation was based on measurements of formation factors and porosities for carbonate rock. He obtained cementation factors of 1.8–2.0. The equation applies only for sediments where the electric current is carried by an electrolytic pore fluid and the grains are insulators. Winsauer et al. (1952) modified Archie's equation to

$$F = \frac{a}{\varphi^m} \tag{2.3}$$

where the a-factor corrects for clay and other conducting minerals.

If a sedimentary rock is partly water saturated, a relationship between degree of water saturation, porosity, resistivity of the pore water, and resistivity of the partly saturated rock is given as

$$S_w^n = \frac{a}{\varphi^m}\frac{R_w}{R_t} \tag{2.4}$$

where n is the saturation exponent and R_t is the resistivity of the partly water-saturated rock. Equation 2.4 can be also rewrite as

$$\sigma = aS_w^n\phi^m\sigma_w \tag{2.5}$$

Where

σ : effective conductivity of the medium (rock)

σ_w : conductivity of the aqueous phase (electrolyte) within the pores

S_w : water saturation

ϕ : % porosity

n : the saturation exponent

m : the cementation exponent

a : a fitting constant

2.2.2) Finite Element Method

The finite element algorithm is used to investigate the effects of mutual induction between multiple buried targets and the host medium. The currents induced in one conductive target will affect the currents flowing in another target via the process of mutual induction. If the host is conductive, currents also flow therein, adding to the complexity of the interaction between targets. The combined effect of these two

processes has been dubbed the “mutual coupling”. The effect of mutual induction between multiple targets is poorly understood, and often the host effect is wholly neglected, largely due to lack of availability of a fully three-dimensional forward modeling code.

Finite Element (FE) method is numerical techniques for solving Maxwell’s diffusion equations in inhomogeneous, electrically conducting media. The two methods are comparable in terms of solution accuracy, storage requirements, and execution speed.

The FE method operates with completely unstructured meshes whose element boundaries can be made to conform to irregular geometries that are characteristic of subsurface heterogeneities, including the deviating boreholes, fluid invasion zones, and dipping geological formations routinely encountered in petroleum well logging. (Wang and Hohmann, 1993; Smith, 1996)

The phenomenon of electromagnetic induction is described concisely by Maxwell’s equations:

$$\nabla \cdot \vec{E} = \frac{1}{\in} \rho \tag{2.6}$$

$$\nabla \cdot H = 0 \tag{2.7}$$

$$\nabla \times \vec{E} = -\mu \frac{\partial H}{\partial t} \tag{2.8}$$

$$\nabla \times \vec{H} = \vec{J} + \in \frac{\partial E}{\partial t} \tag{2.9}$$

where E is the electric field, H is the magnetic field, ρ is the charge density, $\in$ is the electric permittivity, and J is the current density. Several other constitutive relationships constrain these equations:

$$\vec{B} = \mu \vec{H} \tag{2.10}$$

$$\vec{D} = \varepsilon \vec{E} \tag{2.11}$$

$$\vec{J} = \sigma \vec{E} + \vec{J}_s \tag{2.12}$$

where *B* is the magnetic induction, μ is the magnetic permeability, and σ is the conductivity.

The entirety of electrodynamics is described by Maxwell's equations. A more thorough treatment of electrodynamics theory may be found in Griffiths (1999). Gauss's law, equation 2.6, states that an electric field diverges away from a collection of positive charges, and toward a collection of negative charges. Despite diligent investigation, magnetic charges have never been observed in nature. Therefore, all magnetic fields must be divergence-free (equation 2.7). A time-varying magnetic field induces an electric field that curls around the magnetic field. This is Faraday's law (equation 2.8). Magnetic fields curl around current densities, and are induced by time varying electric fields, according to equation 2.9, originally stated by Ampere and revised by Maxwell.

The solution of the secondary coupled-vector potential formulation of Maxwell's equations governing the controlled-source electromagnetic (CSEM) response of an arbitrary, three- dimensional conductivity model must be calculated numerically. The finite element method is attractive, because it allows the model to be discretized into an unstructured mesh, permitting the specification of realistic irregular conductor geometries, and permitting the mesh to be refined locally, where finer resolution is needed. The calculated results for a series of simple test problems, ranging from one-dimensional scalar differential equations to three-dimensional coupled vector equations match the known analytic solutions well, with error values several orders of magnitude smaller than the calculated values. The electro- magnetic fields of a fully three-dimensional CSEM model, recovered from the potentials using the moving least squares interpolation numerical differentiation algorithm, compares well with published numerical modeling results, particularly when local refinement is applied. (Stalnaker, J.L., 2002)

2.2.3) CSEM Method

The theory and practice of the marine CSEM method are fairly well documented. In addition to the references cited in the introduction, we refer the reader to Edwards (2005) and Constable and Weiss (2006). The frequency domain dipole-dipole electric

configuration shown in Figure 1.4 is the method of choice for various reasons (Constable, S. and Srnka, L.J., 2007):

1) An alternative to the frequency-domain approach is the time-domain method, which is well suited to land exploration where the geologic formations are on the conductive side of the air/earth system; after transmitter turn off, the direct wave in the atmosphere dissipates at the speed of light to leave eddy currents propagating more slowly in the ground. On the deep seafloor, the seabed is generally more resistive than seawater, and so information about the geology is embedded in the early time response, whereas the (uninteresting) seawater response dominates late time. In the frequency domain, however, the longer skin depths associated with seafloor rocks mean that at a sufficient source-receiver distance, the field is dominated by energy propagating through the geologic formations. Energy propagating through the seawater has essentially been absorbed and is absent from the signals. Furthermore, by concentrating all the transmitter power into one frequency, larger signal-to-noise ratios can be achieved at larger source-receiver offsets. However, that these are operational considerations, and that the physics of both the time-domain and frequency-domain methods are the same. In principle, a sufficiently broadband frequency-domain survey would be equivalent to a time-domain survey. In practice, a square wave, or other binary switched waveform, is easier to generate than a pure sinusoid for a frequency-domain survey. A square wave has the additional advantage that the fundamental harmonic has an amplitude of $4/\pi$ times the zero to peak current.

2) Electric fields are well suited to operation in seawater. Transmitter currents of 1000A or more can be passed through seawater with simple electrode systems and reasonable power consumption (of order 100 kW), and transmitter antennas several hundred meters long can easily be towed along their length through the seawater. Receiver noise is very low because cultural and MT noise is highly (if not totally) attenuated in the CSEM frequency band. Magnetic field receivers are employed, but motion of the sensors as water currents move the receiver instrument limits the noise

floor. (On land, magnetic sensors are buried to avoid this problem, but they can still be subjected to noise associated with ground motion from trees, microseisms, traffic, etc.)

3) A horizontal electric dipole excites both vertical and horizontal current flow in the seabed, maximizing resolution for a variety of structures. A vertical magnetic dipole, for example, would excite mainly horizontal current flow (Chave et al., 1991).Horizontal magnetic dipoles also excite both vertical and horizontal currents, but are less favored than electric dipoles for operational reasons.

CHAPTER III

METHODOLOGY

The approach taken in this study was the utilization of three software applications. One software application is used for building of the carbonate reservoir, another for analysis of the conductivity model, and the third to simulate CSEM response. The building of the reservoir model was accomplished using the commercially available simulator GEM™, a product of the Computer Modelling Group Ltd. (CMG). GEM™ is a multidimensional, equation of state, compositional simulator capable of modeling carbonate reservoirs. CSEM simulation was done using Finite Element Modeling, developed by Um, Harris and Alumbaugh (2010).

The following flow chart illustrates the order of steps taken.

1. Literature review
    - Study previous works that are related to this project from published papers about the CSEM method, CO_2 sequestration, geological reservoir of Arab-D in Ghawar field, rock physics, and 4-D CSEM modeling.

2. Data collection of the study area
    - Study the necessary parameters given in the papers in order to create the reservoir model of the study area.

3. Build a geological reservoir model
    - Build a geological reservoir model by using Builder software based on the geological parameters of the reservoir from the papers.

4. Run the fluid simulation and rock physics study
    - Use GEM software run model by injecting CO_2 over 10 years in the reservoir, then export time-lapse rock properties and convert to electrical properties.

5. Compute CSEM time-lapse simulation by using a finite element modeling

    - Apply a finite element modeling (Badea et al, 2001) to compute CSEM time-lapse simulation.

6. Interpretation CSEM responses

    - Collect and interpret time-lapse CSEM responses from the laboratory.

7. Make a discussion and conclusion.

    - Discuss and conclude of all results for leading to presentation and report.

8. Make report and present the entire project.

    - In the final step the report is written and submitted to the Department.
    - Prepare presentation seminar on senior projects of the department.

Methods of study can be summarized in the schematic diagram (Figure 3.1) and detail is described below.

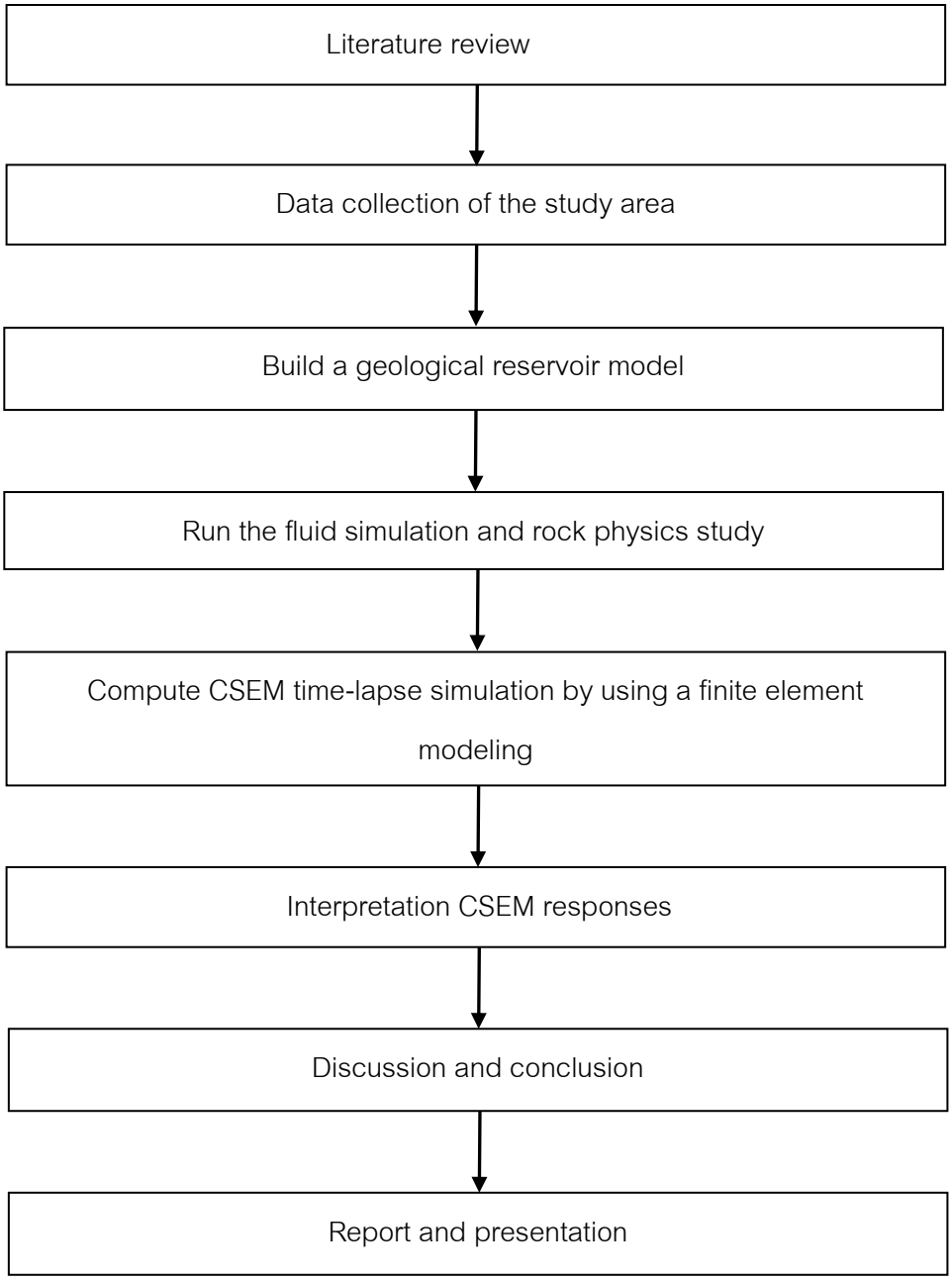

Figure 3.1: Schematic diagram showing study steps of the research project.

CHAPTER IV

RESULTS AND INTERPRETATION

4.1 Data Collection of the Study Area

To study the CSEM response due to CO_2 injection, I demonstrate the CSEM response of a carbonate reservoir in Ghawar field, Saudi Arabia which is acquire the data of the location from available research, Origin of Dolomite in the Arab-D Reservoir from the Ghawar Field, Saudi Arabia: Evidence from Petrographic and Geochemical Constraints (Swart et al., 2005) (Figure 4.1).

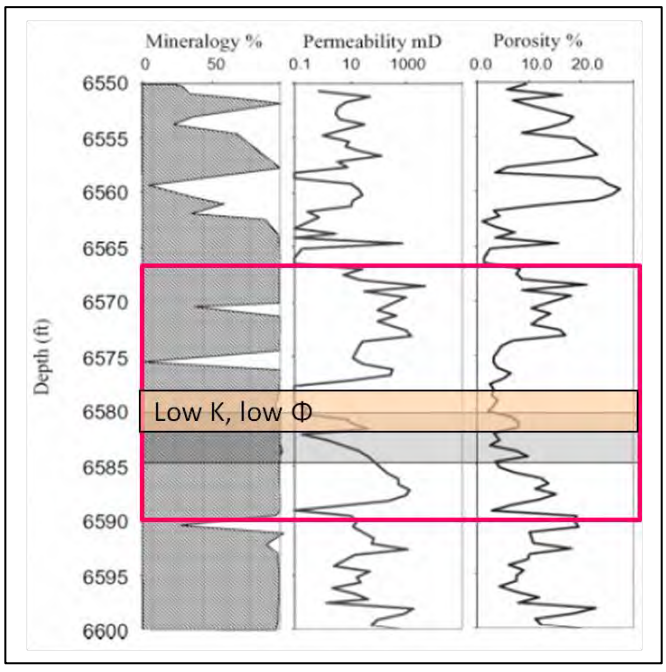

Figure 4.1: Well log data from the available research (Swart et al., 2005). Red box indicates data used to construct our geologic model.

4.2 Geological Reservoir Model

I constructed the model using porosity and permeability data from a carbonate reservoir in the Ghawar oil field, Saudia Arabia (Swart et al., 2005) by using CMG

Technologies which provides Builder software in order to build the model. To build up the model, I had to integrate both structural and physical properties of the reservoir.

The geological model composed of 15 layers with different physical properties such as porosity, permeability (Figure 4.2). The pressure in the model was defined at 2000kPa. Then I defined initial composition of the reservoir to be 1% CO_2 and 99% water for the whole layers.

General Property Specification

dit Specification

Go To Property: Permeability K | Use Regions / Sectors

	Grid Top	Grid Thickness	Porosity	Permeability I	Permeability J	Permeability K
UNITS:	m	m		md	md	md
SPECIFIED:		X	X	X	X	X
HAS VALUES:	X	X	X	X	X	X
Whole Grid		10				
Layer 1			0.02	0.0001	0.0001	0.0004
Layer 2			0.05	20	20	9
Layer 3			0.22	5000	5000	2222
Layer 4			0.15	785	785	350
Layer 5			0.04	11	11	5
Layer 6			0.04	130	130	58
Layer 7			0.04	125	125	56
Layer 8			0.03	0.0001	0.0001	0.0004
Layer 9			0.03	0.1	0.1	0.04
Layer 10			0.05	5	5	2.2
Layer 11			0.08	20	20	9
Layer 12			0.04	3	3	0.2
Layer 13			0.07	40	40	18
Layer 14			0.11	530	530	24
Layer 15			0.02	0.0001	0.0001	0.0004

Figure 4.2: The general property specification of the model with different porosity and permeability of each layer.

Size of the model is 600m x 600m x 150m. The geologic model is composed of 15 layers of 10m thickness each. I inserted 12 producing well around the model with 1 injection well with pressure 5000kPa (Figure 4.3).

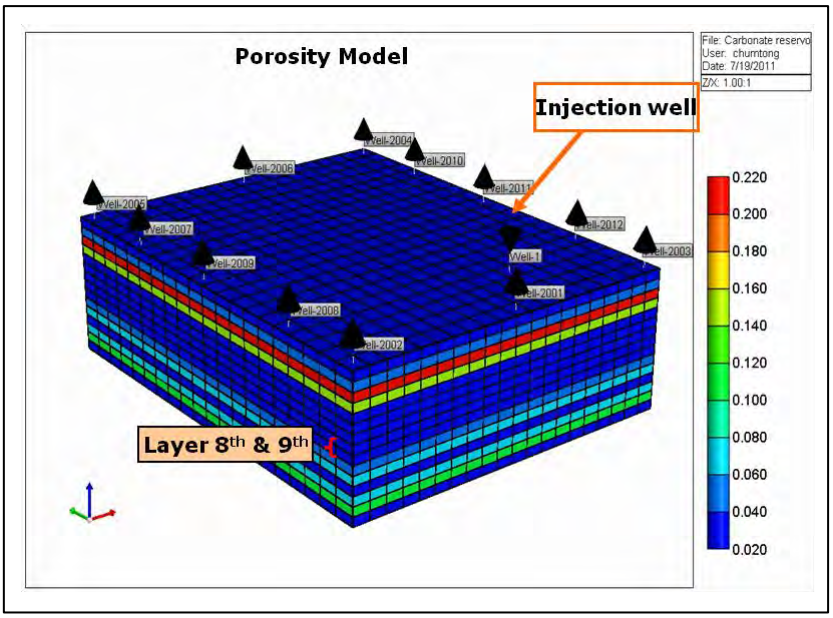

Figure 4.3: The constructed geological reservoir model.

Then GEM software was used to run the simulation of injecting CO_2. After trying to inject CO_2 into the second layer from bottom, I found that there are 2 low porosity and low permeability layers at the middle layers of the reservoir which CO_2 could not get through these layers. Therefore, I inserted two cracks into these layers indicated by orange box (Figure 4.4). The cracks components are composed of 100md of I and J permeability and 50md of K permeability.

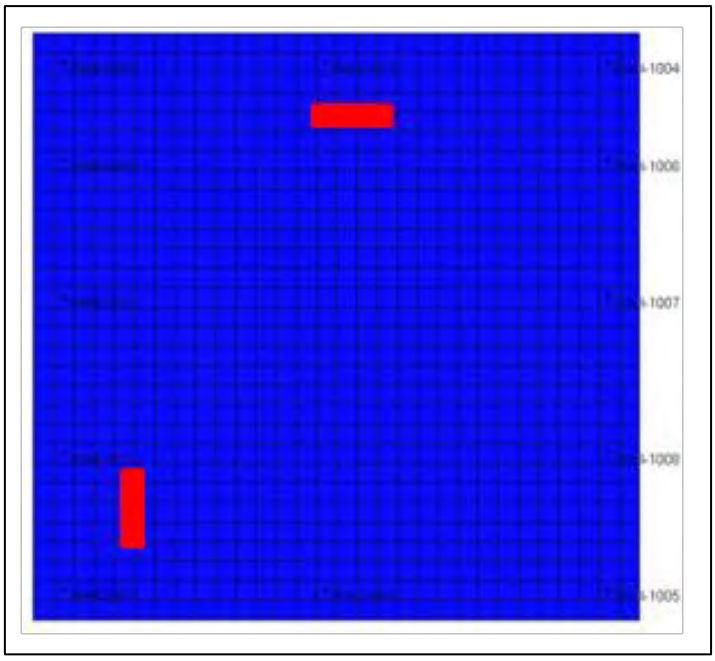

Figure 4.4: The two inserted cracks in the eighth and ninth layers which are indicated by red boxes.

4.3 Flow Simulation

After I built the model, I used GEM software to run the model by injecting CO_2 over 10 years in the reservoir. CO_2 was injected into the 14^{th} layer from the top (Figure 4.5).

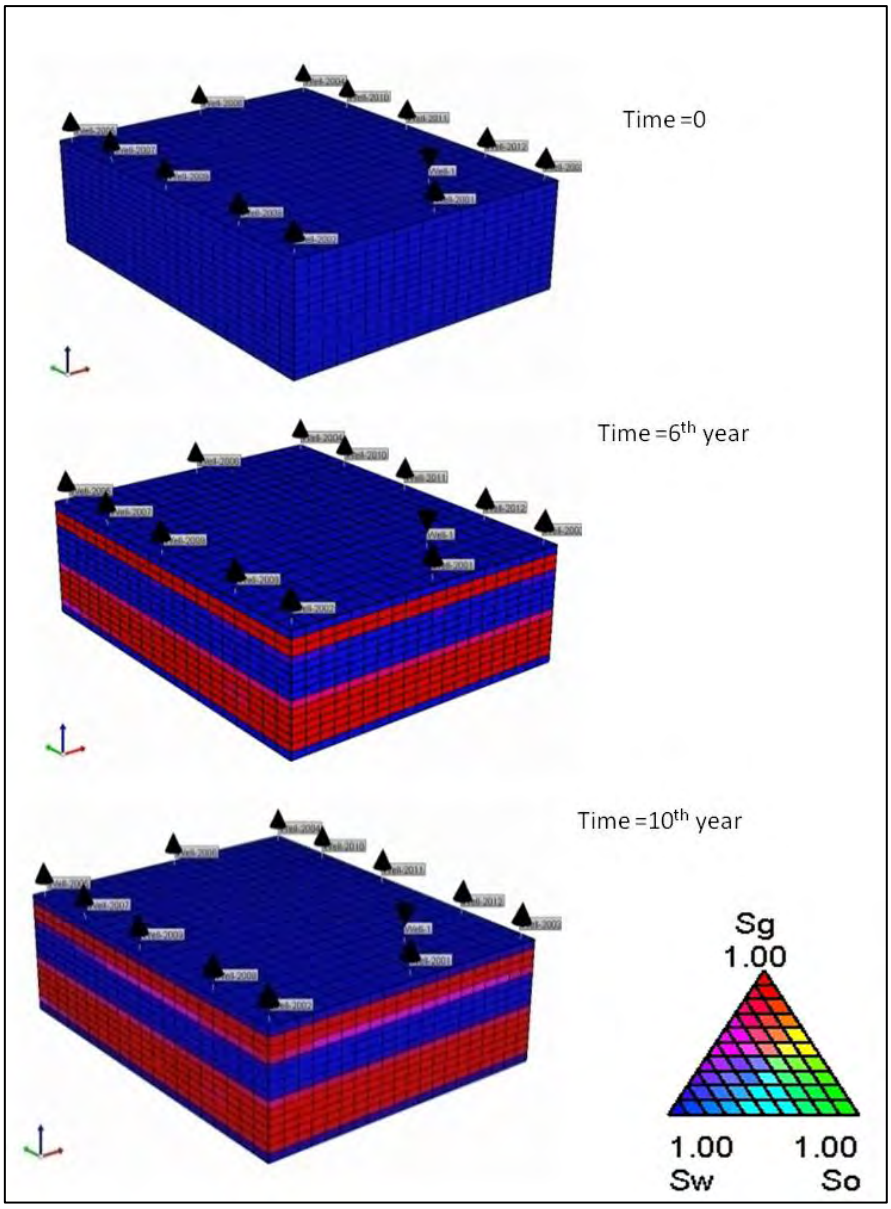

Figure 4.5: Time lapse reservoir response to CO_2 injection at 0, 6, and 10 years.

As shown in Figure 4.5, the triangular color scale represents the composition and saturation of model elements. After 6 years, CO_2 has spread through the deep high permeability layers as well as through the cracks to layers near the surface. CO_2 has yet to fill the middle, low permeability layers. After 10 years of injection, CO_2 has begun to migrate down into the lower permeability layers.

4.4 Rock Physics Study

Rock physics is the study of relationships between rock properties and geophysical observation (i.e. CSEM). After running the flow simulation, export water saturation and porosity data of the reservoir at each time lapse. Then, rock physics is used to study the relationship between rock properties and electrical properties (Figure 4.6).

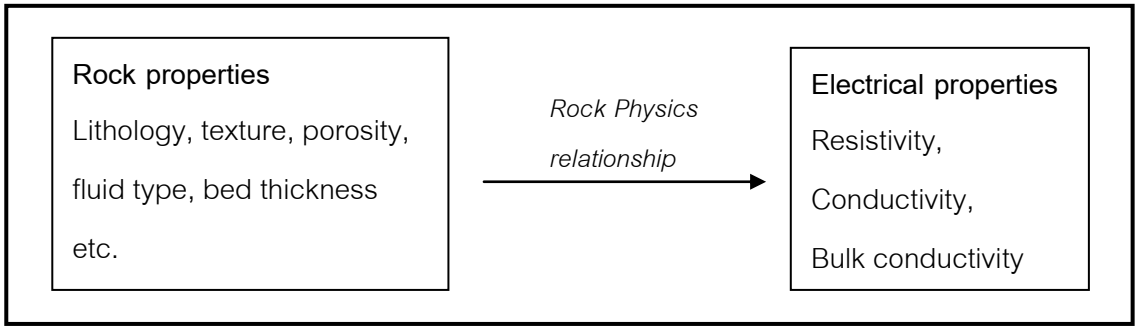

Figure 4.6: Rock physics relationship between rock properties and electrical properties.

To calculate the elastic reservoir model, I applied Archie's law, which is a function of conductivity, water saturation and porosity.

$$\sigma = aS_w{}^n \phi^m \sigma_w \qquad \text{(Archie's law)}$$

By using MatLab software, I input the porosity and water saturation file into the equation, and we finally got the conductivity reservoir model at each time lapse.

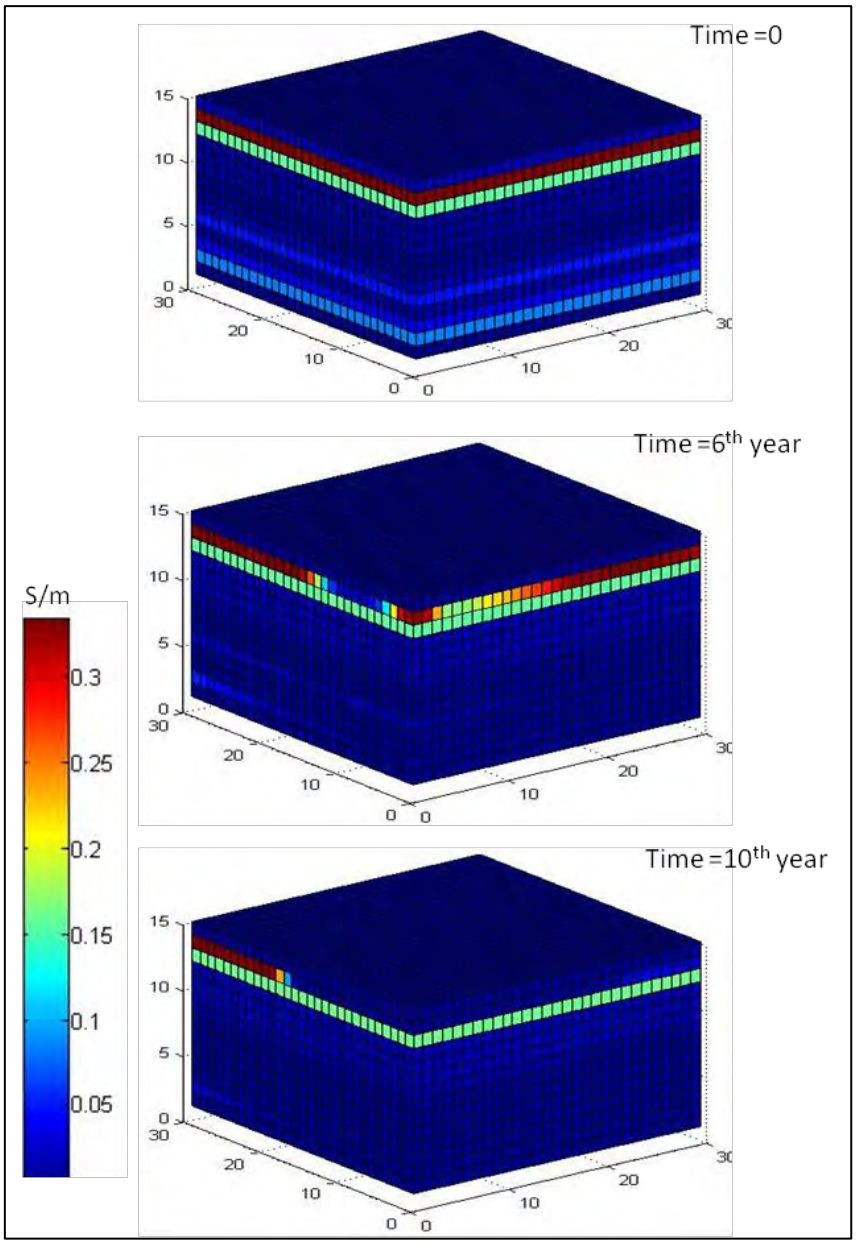

Figure 4.7: The conductivity models at 0, 6, and 10 years.

With the saturation output from fluid simulation, we use Archie's law to calculate the conductivity model at each time lapse. The conductivity models shown here (Figure 4.7) represent the expected changes in conductivity due to CO_2 injection and migration. Color bar indicates conductivity in SI unit (Siemens/meter).

4.5 CSEM Simulation

To simulate an actual marine CSEM survey, the reservoir is buried in a 3D homogenous seabed. The receivers lie on the seafloor above the reservoir location, and the source is an electric dipole oriented along the x-axis (Figure 4.8). A finite element modeling method was used (Um, Harris and Alumbaugh, 2010) to calculate synthetic time-lapse CSEM data over the reservoir.

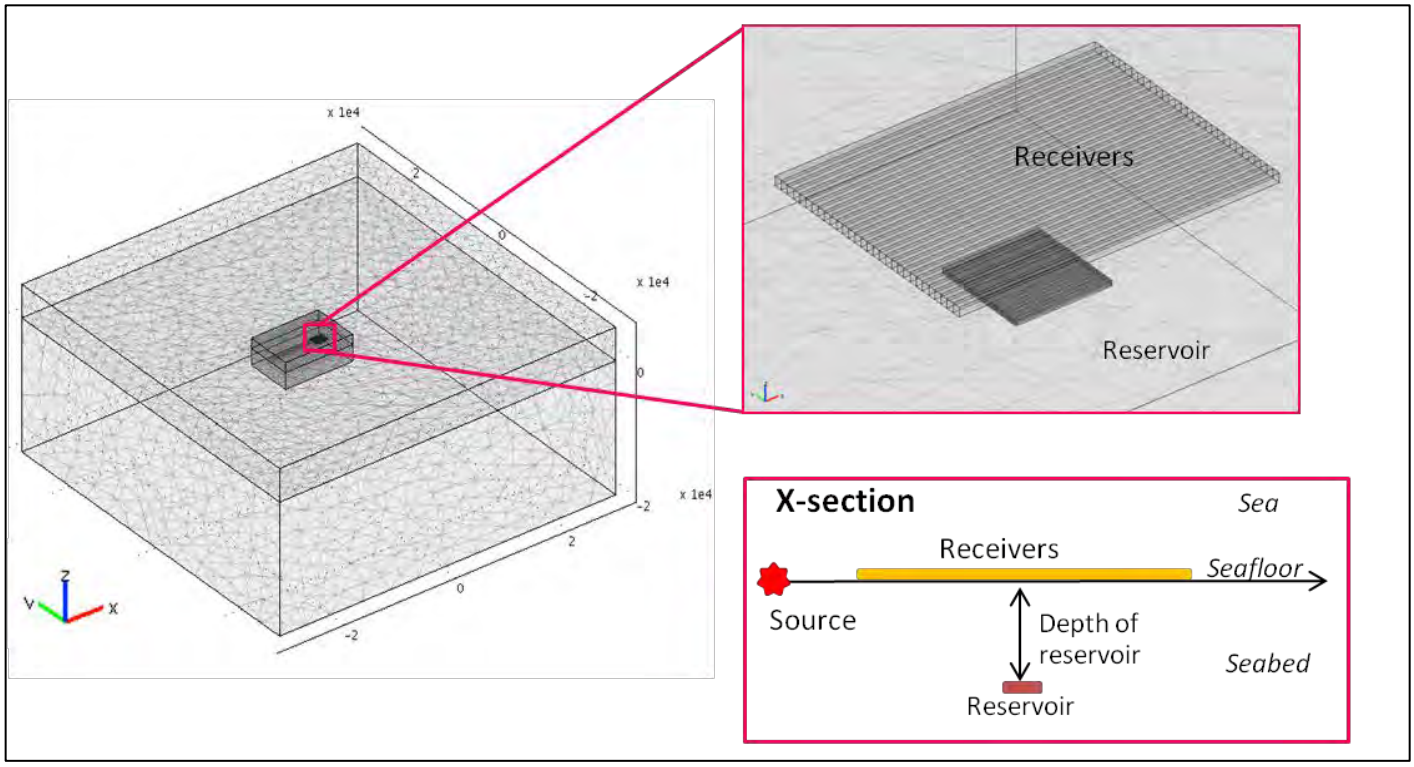

Figure 4.8: Finite element modeling is used to obtain the electromagnetic field of the reservoir.

The reservoir is buried in the homogeneous seabed (Figure 4.8, left). Zoom out figure shows the reservoir-receiver geometry (Figure 4.8, right, top). Cross-section shows the geometry between the source, receivers, and reservoir (Figure 4.8, right, bottom). The receiver array is on the seafloor and above the reservoir. The source is located 4.1 km from the center of the receivers array, and 50m above the seafloor. CSEM data is simulated for various reservoir depths, and source frequencies.

4.6 Computed CSEM Time-Lapse

The results are displayed as normalize differences of the electric field components relative to the initial (baseline survey) components. In the plots that follow, we show the ratio of each component in each axis which is the most robust, as well as resistive and easier to interpret.

Amplitude ratio of $\frac{Ez(t_i) - Ez(t_0)}{Ex(t_0)}$ is calculated and displayed as the results, where

$Ez(t_i)$: Vertical electromagnetic component at interested time (t=i)

$Ez(t_0)$: Vertical electromagnetic component at initial time (t=0)

$Ex(t_0)$: Horizontal electromagnetic component at initial time (t=0)

From the ratio above, the results will tell about relative change of electromagnetic due to changes in saturation within the reservoir.

4.6.1) Given Frequency Comparison

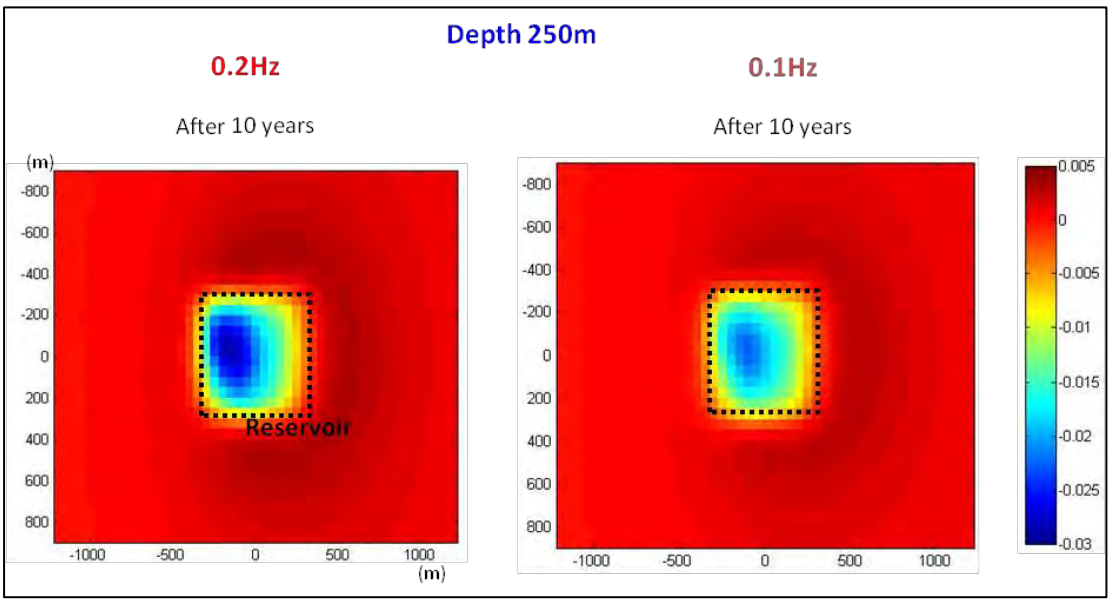

Figure 4.9: Comparison of different source frequency at reservoir depth 250m.

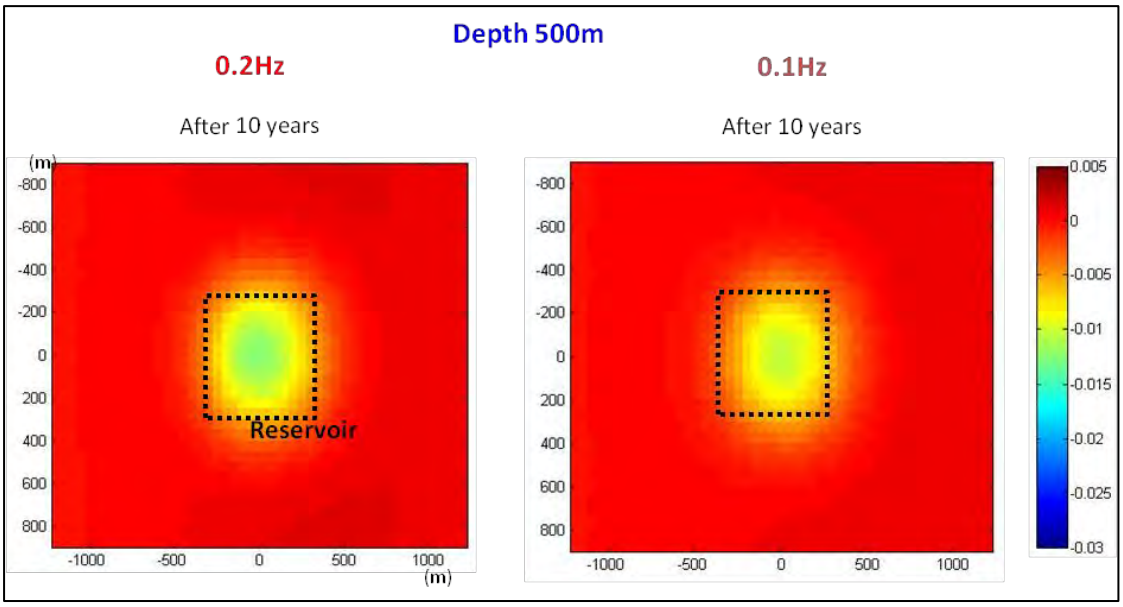

Figure 4.10: Comparison of different source frequency at reservoir depth 500m.

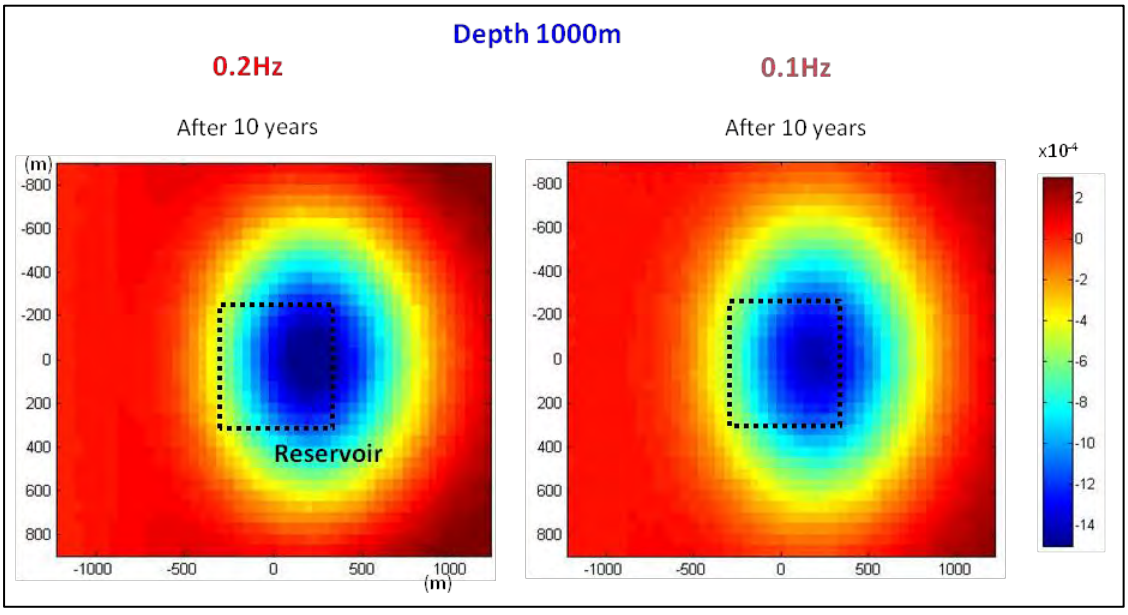

Figure 4.11: Comparison of different source frequency at reservoir depth 1000m. Note that changes in color scale at 1000m.

Figure 4.9, Figure 4.10,and Figure 4.11 above show synthetic CSEM data (amplitude ratio) for the reservoir at the end of the fluid flow simulation calculated for

sources at 0.2 Hz (left) and 0.1 Hz (right) at depths of 250m (Figure 4.9), 500m (Figure4.10), and 1000m (Figure 4.11). Note that changes in color scale at 1000m.

You can notice that higher frequencies give higher resolution, and resolution decreases with depth. Furthermore, the width of the anomaly increases when the depth of the reservoir increases.

4.6.2) At depth 250m and 1000m Comparison

We first recognize changes in the reservoir as shown in figure 4.12 below.

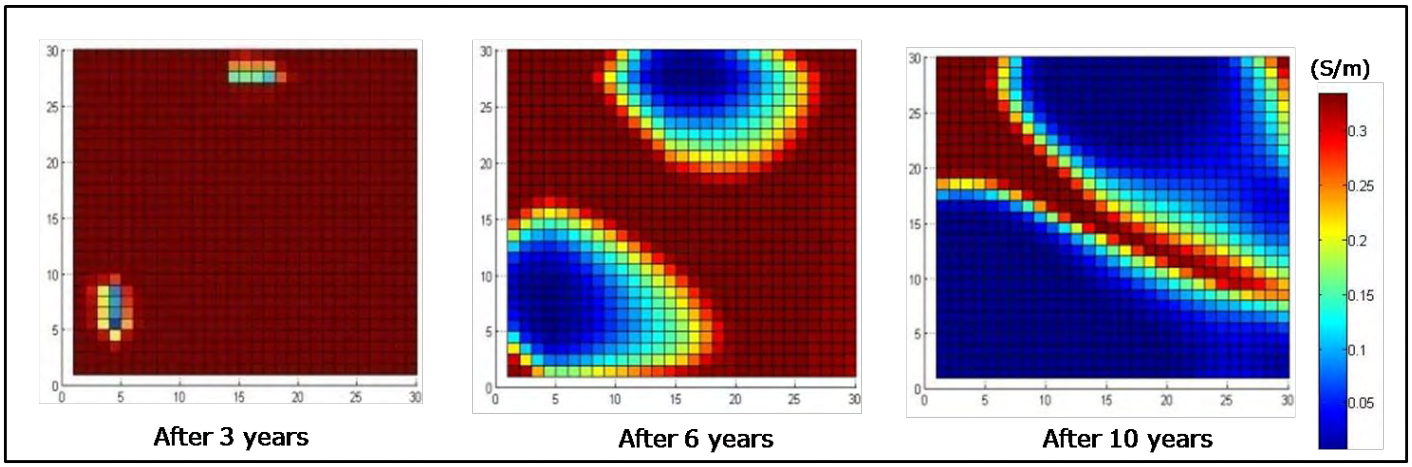

Figure 4.12: Plain view of the reservoir conductivity after 3 years (left), 6 years (middle), and 10 years (right) of CO_2 injection.

The change of conductivity in the reservoir relates to crack locations that have been created at the lower layers in the reservoir. Conductivity decreases because CO_2 is resistive while water is conductive.

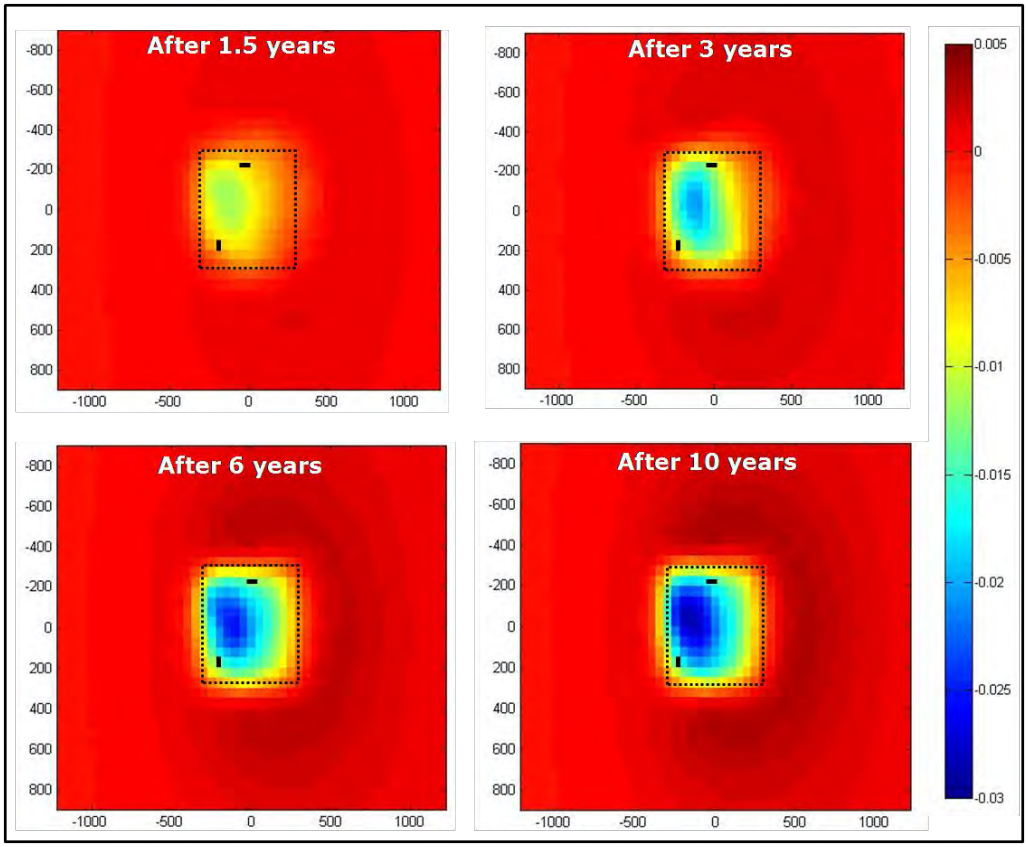

Figure 4.13: Synthetic CSEM data (amplitude ratio) for the reservoir at the end of the fluid flow simulation calculated for sources at 0.2 at depths of 250m at four time-lapse.

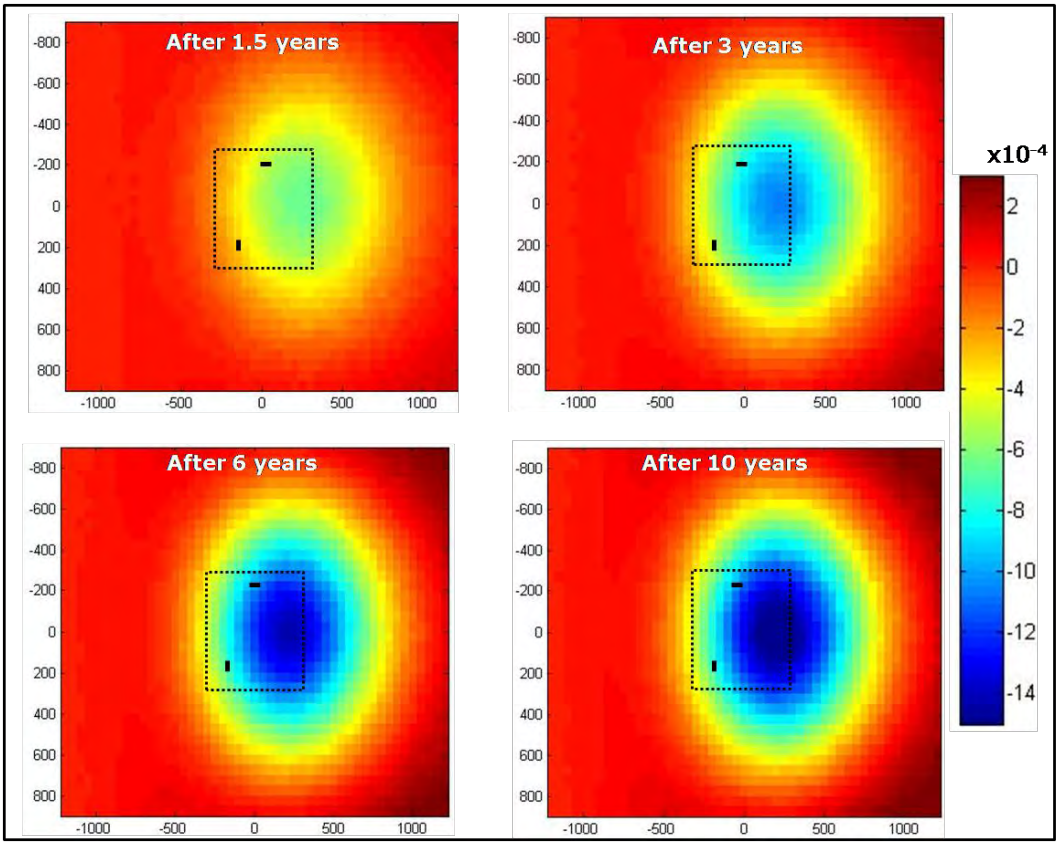

Figure 4.14: Synthetic CSEM data (amplitude ratio) for the reservoir at the end of the fluid flow simulation calculated for sources at 0.2 at depths of 1000m at four time-lapse.

At 250m depth (Figure 4.13), we can observe distinct anomalies in reservoir conductivity after 1.5 years. Further, the anomalies correlate to the location of the cracks within the reservoir (Figure 4.12). At 1000m depth (Figure 4.14), the anomaly has a small magnitude which would be hard to detect in practice, and the location is not exactly on top of the region where the changes of conductivity are occurring.

CHAPTER V

CONCLUSION

1. CSEM can measure changes associated with fluid flow within carbonate reservoirs.

2. For shallow reservoirs (depth < 500 m), CSEM can detect a change from unsaturated conditions after 1.5 years.

3. Deeper (1000 m) reservoirs require long time periods (>= 10 years) before saturation changes can be noticed. However, the relative changes are smaller than 1%.

4. Anomaly resolution decreases with depth

5. It is preferable to use higher frequency sources in order to obtain a better resolution.

6. An inversion of CSEM data will allow us to improve its interpretation.

References

Archie, G.E., 1942, The electrical resistivity log as an aid to determining some reservoir characteristics: Transactions of the American Institute of Mining and Metallurgical Engineers, 146, 54–62.

Badea, E. A., Everett, M.E., Newman, G.A., and Biro, O., 2001, Finite-element analysis of controlled-source electromagnetic induction using Coulomb- gauged potentials: Geophysics, 66, 786–799.

Constable, S., and Weiss, C. J., 2006, Mapping thin resistors and hydrocarbons with marine EM methods: Insights from 1D modeling: Geophysics, 71, no. 2, G43–G51.

Constable, S., and Srnka, L.J., 2007, An introduction to marine controlled-source electromagnetic methods for hydrocarbon exploration: Geophysics, 72, no. 2, P. WA3–WA12, 6 FIGS.

Davis, T., 2010, The State of EOR with CO2 and associated seismic monitoring: The Leading edge, 29, 31-33.

Durham, L.S., 2005, The elephant of all elephants: American Association of Petroleum Geologists, Explorer, 26, 4–7.

Edidesmo, T., Ellingsrud, S., MacGregor, L.M., Constable, S., Sinha M.C., Johanson, S., Kong, F.N., and Westerdahl, H., 2002, Sea bed logging SBL, a new method for remote and direct identification of hydrocarbon filled layers in deepwater areas: First Break, 20, 144–152.

EPA, 2007, Atmosphere Changes, U.S. Environmental Protection Agency and the Gas Research Institute, Washington, D.C. (Website: http://www.epa.gov/climatechange /science/recentac.html).

Eugene, A.B., Everett, M.E., and Newman, G.A., 2001, Finite-element analysis of controlled-source electromagnetic induction using Coulomb-gauged potentials: Geophysics, 66, no. 3, 786–799.

Grant, F., and West, G., 1965, Interpretation theory in applied geophysics, International Series in the Earth Sciences: McGraw-Hill Book Company.

Lien, M., and Mannseth, T., 2008, Sensitivity study of marine CSEM data for reservoir production monitoring: Geophysics, 73, no. 4, F151–F163.

Michael, A.F. and Davydycheva, S., 2009, A modeling study of low-frequency csem in shallow water, 71st EAGE Conference & Exhibition — Amsterdam, The Netherlands, 8 - 11 June 2009.

Smith, J.T., 1996, Conservative modeling of 3-D electromagnetic fields: Geophysics, 61, 1308–1324.

Stalnaker, J.L. and Everett, M.E., 2002, Finite element analysis of controlled-source electromagnetic induction for near-surface geophysical prospecting: The 16thWorkshop on Electromagnetic Induction in the Earth, Santa Fe, NM, EM 5-40.

Swart, P.K., Cantrell, D.L., Westphal, H., Handford, C.R., and Kendall, C.G., 2005. Origin of dolomite in the Arab-D reservoir from the Ghawar field, Saudi Arabia: Evidence from geochemical and petrographic constraints, Journal of Sedimentary Research, 75, 476-491.

Wang, T., and Hohmann, G.W., 1993, A finite-difference time-domain solution for three-dimensional electromagnetic modeling: Geophysics, 58, 797–809.

Wright, D., Ziolkowski, A., and Hobbs, B., 2002, Hydrocarbon detection and monitoring with a multicomponent transient electromagnetic (MTEM) survey: The Leading Edge, 21, no. 9, 852-864.